HF RADIO CHANNEL MODELING BY A WAVEGUIDE APPROACH

V.I. Kurkin
Institute of Solar-Terrestrial Physics SB RAS,
Irkutsk, Russia, kurkin@iszf.irk.ru

N.V. Ilyin
Institute of Solar-Terrestrial Physics SB RAS,
Irkutsk, Russia, ilyin@iszf.irk.ru

M.S. Penzin
Institute of Solar-Terrestrial Physics SB RAS,
Irkutsk, Russia, penzin.maksim@gmail.com

S.N. Ponomarchuk
Institute of Solar-Terrestrial Physics SB RAS,
Irkutsk, Russia, spon@iszf.irk.ru

V.V. Khakhinov
Institute of Solar-Terrestrial Physics SB RAS,
Irkutsk, Russia, khakhin@iszf.irk.ru

Abstract. We present a modified method of HF radio channel modeling based on a waveguide approach. The waveguide approach represents the electromagnetic field of radiation inside the Earth—ionosphere waveguide as an eigenfunction series of a radial boundary problem with impedance conditions on the Earth surface and radiation conditions at infinity. The transfer function of the radio channel is represented as a series of products of angular-operator Green functions, excitation coefficients, and coefficients for receiving individual normal modes. We have obtained a solution of the boundary value problem of determining the eigenfunc-tions and eigenvalues of the radial operator. The solution can be applied to the frequency range below the ionospheric F-layer critical frequency. We examine algorithms for calculating distance-frequency, frequency-angular, and amplitude characteristics of signals by analyzing and numerically summarizing the series in terms of strongly damped normal modes.

Keywords: radio wave propagation, radio channel, waveguide approach, simulation, ionosphere sounding.

INTRODUCTION

The decameter range is widely used for developing various radio engineering systems due to the capability of providing conditions for communication and radar over long distances, as well as for diagnostics of the environment in large spatial areas. For such systems to operate, it is important to devise effective computational schemes for modeling the characteristics of radio wave propagation along long and ultra-long radio paths. Methods for calculating HF propagation characteristics were developed most intensively in the 1970s–1980s. Approaches based on the geometrical optics method were generally adopted [Kazantsev et al., 1967; Lukin, Spiridonov, 1969; Kravtsov, Orlov, 1980], which could calculate the trajectory characteristics of propagation and estimate the amplitude of a signal. Studies were also carried out which delved into radio wave propagation, development of effective methods for calculating various HF-signal characteristics for models close to real propagation conditions. The adiabatic invariant method [Gurevich, Tsedilina, 1979] and its generalizations based on asymptotic solutions of ray equations [Baranov et al., 1992] increased the efficiency of the analysis of long-range radio paths. Numerical methods applying the Maslov canonical operator [Ipatov et al., 1990] and the theory of catastrophes [Kryukovskii et al., 2006] made it possible to analyze the field in an inhomogeneous magnetoactive medium, taking into account peculiarities in caustics [Ipatov et al., 2014]. The effects of the influence of random irregularities of various scales were studied using the interference integral method [Avdeev et al., 1988] and the generalization of the Rytov method [Zernov et al., 1992]. The parabolic equation method was also applied to these problems [Cherkashin, 1971; Baranov, Popov, 1993].

Another approach to the description of long-range HF radio wave propagation is the waveguide approach — the method of normal modes proposed by P.E. Krasnushkin in 1947 [Krasnushkin, 1947] and developed in the 1980s by the team of researchers led by I.I. Orlov [Kurkin et al., 1981]. The method is one of the main ones in the range of very long waves [Krasnushkin, Yablochkin, 1963; Makarov et al., 1993] and in underwater acoustics [Ahluwalia, Keller, 1980; Kamel, Felsen, 1982]. In the waveguide approach, the HF electromagnetic field inside the Earth—ionosphere waveguide is represented as an eigenfunction series of the radial boundary value problem [Kurkin et al., 1981]. For the numerical implementation of the method, the series is limited to a group of normal modes effectively excited by the transmitter and weakly decaying. When solving the unified electrodynamic problem of radio wave transmission, propagation, and reception, the waveguide approach is used to obtain expressions for excitation and reception coefficients of normal modes [Kurkin, Khakhinov, 1984; Khakhinov, 2018] for antennas of standard types employed in HF radio communications [Aizenberg et al., 1985]. Using the mathematical scheme of analysis and numerical summation of a number of normal modes, algorithms for modeling the main HF signal characteristics were implemented without complicating calculations in terms of signal focusing at the skip zone border [Kurkin et al., 1982].

Modern HF radio communication, including cognitive radio, involves adjusting radio equipment parameters for changing radio path properties, using data from active and passive ionospheric sounding [Anderson, 2019; Ayliffe et al., 2019]. The methods of adapting radio system parameters are generally based on the analysis of the radio-channel transfer function by applying models of radio wave transmission, reception, and propagation in the ionosphere. Receiver radio signal processing matched to the transmitted signal makes it possible to eliminate received-signal distortions introduced by the transfer function of the real radio channel [Ivanov et al., 2019a, b]. Operating radio frequencies are selected based on the signal-to-noise ratio, taking into account multipath propagation of the recorded signal. As an example of constructing a transfer function by the geometrical optics method, we can point to the dynamic adaptive physically structural model of ionospheric radio channel developed at Rostov State University [Barabashov, Vertogradov, 1996].

In general, an HF radio channel includes a set of devices used to transmit information from a source to a receiver, and a radio wave propagation medium. Structure flowchart of an HF radio channel is shown in Figure 1. We examine a radio channel with known technical and functional characteristics of its constituent parts: receiving-transmitting antenna-feeder systems, the Earth—ionosphere waveguide. It is expected that the transmitting and receiving devices are coordinated with transmitting and receiving antennas and there is no loss of signal energy in antenna feeders. The ionosphere is considered stationary during signal propagation from a transmitter to a receiver.

The paper presents a composite model of HF radio channel, including transmitting and receiving devices, an ionospheric radio channel, and a software package for calculating characteristics of radio signals by the method of normal modes. In the first part of the work, we introduce a scheme for framing a solution of Maxwell equations for the electromagnetic field components in the inhomogeneous Earth—ionosphere waveguide as an expansion in radial-operator eigenfunctions. In the second part, we construct solutions of the radial boundary value problem for eigenfunctions and eigenvalues, tak-

ing into account signal field absorption in the ionosphere and on Earth surface for the decameter frequency range, including frequencies below the F-layer critical frequency. Then, we present a scheme for constructing the transfer function of an ionospheric radio channel as a series of products of angular-operator Green functions, excitation coefficients, receiving coefficients of individual normal modes, which depend on eigenfunctions and eigenvalues of the radial boundary value problem in terms of strongly damped waveguide modes. We introduce a scheme for processing quasi-monochromatic signals and signals with linear frequency modulation (chirp signals). We examine algorithms for numerical modeling of HF-signal distance and amplitude characteristics by analyzing and numerically summing a number of normal modes. In the final part of the work, we present the results of numerical simulation of radio signal characteristics with the developed software package. The developed methods and algorithms enable both rapid calculations within a two-point formulation of the problem for HF radio paths and simulation of spatial distributions of radiation on the Earth surface or its vertical distributions in the Earth—ionosphere waveguide at different ranges from the transmitter.

METHOD OF NORMAL MODES

The waveguide approach solves a single electrodynamic problem of radio wave transmission, propagation, and reception. Let us examine a scheme for constructing a solution of Maxwell equations by the method of normal modes in the isotropic azimuthally symmetric Earth—ionosphere waveguide. The polar axis of the spherical coordinate system passes through a transmitting system. For the Fourier components of the electromagnetic field with harmonic dependence on time $\exp(-i\omega t)$ the Maxwell equations can be written as:

$$\text{rot } \vec{B} = -ik\hat{\varepsilon}\vec{E} + \frac{4\pi}{\omega}\vec{j}, \text{ rot } \vec{E} = ik\vec{B}. \tag{1}$$

The complex permittivity of the ionosphere $\hat{\varepsilon}$ in the cold plasma approximation has the form [Ginzburg, 1967]
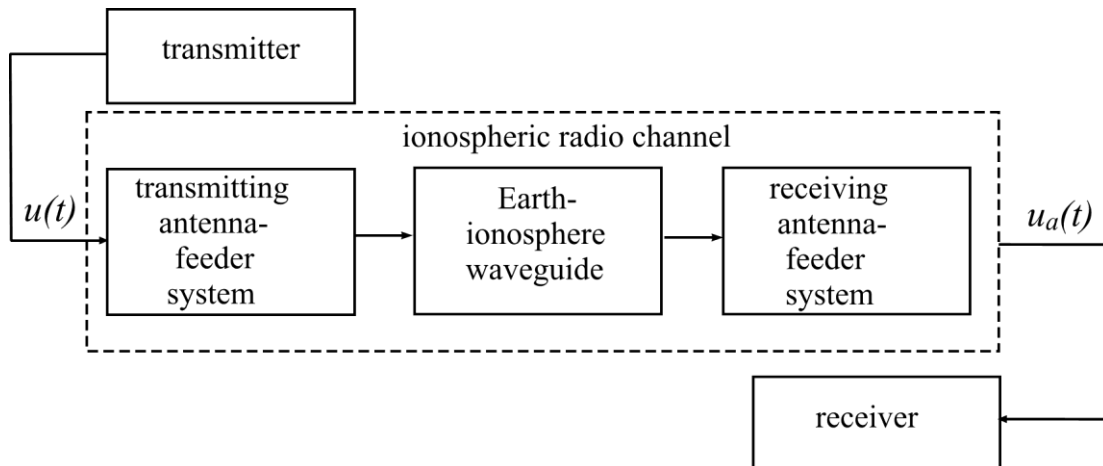

Figure 1. Structure flowchart of an HF radio channel

$$\hat{\varepsilon}(r,\theta,\omega) = \varepsilon(r,\theta,\omega) +$$

$$+i\varepsilon''(r,\theta,\omega) = 1 - \frac{4\pi e^2 N(r,\theta)}{m\omega\left[\omega + iv_{\text{eff}}(r,\theta)\right]}. \qquad (2)$$

Inside Earth, $0 < r \le a$, where a is the Earth radius, $\hat{\varepsilon} = \hat{\varepsilon}_t = \varepsilon_t + i\dfrac{4\pi}{\omega}\sigma_t$; in the region $a < r < r_H$, where r_H is the coordinate of the lower boundary of the ionosphere, $\hat{\varepsilon}=1$; at infinity $\lim\limits_{r\to\infty}\hat{\varepsilon} = 1$. The boundary conditions on the surface $r = a$ for $\vec{E}, \vec{B}$ have the form

$$\vec{B}_t = \vec{B}, \ E_{t\varphi}=E_\varphi, \ E_{t\theta}=E_\theta, \ \hat{\varepsilon}_t E_{tr} = E_r. \qquad (3)$$

The index t in (3) refers to the field inside Earth. At infinity, the fields should satisfy the radiation condition

$$\lim_{r\to\infty}\left(\frac{\partial(r\vec{E})}{\partial r} - ik\vec{E}\right) = 0,$$

$$\lim_{r\to\infty}\left(\frac{\partial(r\vec{B})}{\partial r} - ik\vec{B}\right) = 0. \qquad (4)$$

In (1) and (4), $k = \omega/c$. If the current density in (1) $\vec{j}(r,\theta,\omega)$, then, due to the symmetry of the problem with respect to rotations around the polar axis, system of equations (1) is divided into two groups of equations: 1) E_r, E_θ, B_φ form a TM field; 2) B_r, B_θ, E_φ form a TE field. In this case, E_r, E_θ are expressed in terms of B_φ; and B_r, B_θ, in terms of E_φ. Matching conditions for E_φ, B_φ on the surface $r=a$ have the form

$$E_{t\varphi} = E_\varphi, \ \frac{\partial}{\partial r}(rE_{t\varphi}) = \frac{\partial}{\partial r}(rE_\varphi),$$

$$B_{t\varphi} = B_\varphi, \ \frac{1}{\hat{\varepsilon}_t}\frac{\partial}{\partial r}(rB_{t\varphi}) = \frac{\partial}{\partial r}(rB_\varphi). \qquad (5)$$

The general equation for determining E_φ, B_φ after the transition to a new variable $x = -\cos\theta$ and new functions $\tilde{E} = rE_\varphi\sqrt{1-x^2}$ and $\tilde{B} = rB_\varphi\sqrt{1-x^2}/\sqrt{\varepsilon}$ can be written as

$$\frac{\partial^2 \Pi}{\partial r^2} + \tilde{k}^2(r,x)\Pi + \frac{1-x^2}{r^2}\left(\frac{\partial^2 \Pi}{\partial x^2} - \xi(r,x)\Pi\right) =$$

$$= \sqrt{1-x^2}\,\tilde{I}(r,x). \qquad (6)$$

For $\Pi = \tilde{E}$:

$$\tilde{k}^2 = k^2\hat{\varepsilon}, \ \xi = 0, \ \tilde{I} = -ikr\frac{4\pi}{c}j_\varphi.$$

For $\Pi = \tilde{B}$,

$$\tilde{k}^2 = k^2\hat{\varepsilon} - \sqrt{\hat{\varepsilon}}\,\frac{\partial^2}{\partial r^2}\left(\frac{1}{\sqrt{\hat{\varepsilon}}}\right), \ \xi = \sqrt{\hat{\varepsilon}}\,\frac{\partial^2}{\partial x^2}\left(\frac{1}{\sqrt{\hat{\varepsilon}}}\right),$$

$$\tilde{I} = -ikr\frac{4\pi}{c}\text{rot}_\varphi\frac{\vec{j}}{\hat{\varepsilon}}.$$

Conditions (5) take the form

$$\tilde{E}_t = \tilde{E}, \ \frac{\partial \tilde{E}_t}{\partial r} = \frac{\partial \tilde{E}}{\partial r}, \ \sqrt{\hat{\varepsilon}_t}\,\tilde{B}_t = \tilde{B},$$

$$\frac{1}{\hat{\varepsilon}_t}\frac{\partial}{\partial r}\left(\sqrt{\hat{\varepsilon}_t}\,\tilde{B}_t\right) = \frac{\partial \tilde{B}}{\partial r}. \qquad (7)$$

At infinity, the function Π satisfies the radiation condition

$$\lim_{r\to\infty}\left(\frac{\partial \Pi}{\partial r} - ik\Pi\right) = 0. \qquad (8)$$

Represent the solutions of boundary value problems (6)–(8) for $\tilde{E}$ and $\tilde{B}$ at each x as eigenfunction expansion of radial boundary value problems for TM and TE fields, formulated in [Kurkin et al., 1981] for the spherically symmetric waveguide. The radial equation has the form

$$\frac{\partial^2 R_n}{\partial r^2} + \left(\tilde{k}^2(r,x) - \frac{\vartheta_n^2(x)}{r^2}\right)R_n = 0. \qquad (9)$$

Here, ϑ_n^2 is a complex eigenvalue of the radial problem. The boundary conditions for the eigenfunctions R_n on $r=a$ and at infinity are similar to (7) and (8) if R_n is substituted for $\tilde{E}$ and $\tilde{B}$. If we impose the condition that the functions R_n for $r\to 0$ satisfy the relation

$$\lim_{r\to 0}\left(R_n/\sqrt{r}\right) = 0, \qquad (10)$$

for the discrete part of the spectrum of the boundary value problem the radial functions meet the normalization condition [Kurkin et al., 1981]

$$\int_0^\infty \frac{R_n R_m}{r^2}\,dr = \frac{\delta_{nm}}{a}. \qquad (11)$$

Thus, we will seek the solution of (6) in expanded form

$$\Pi(r,x) = \sum_n X_n(x)R_n(r,x). \qquad (12)$$

Insert (12) into (6), multiply by R_m, and integrate over r. This yields

$$X_m'' + \left(\frac{\vartheta_m^2}{1-x^2} - \xi\right)X_m +$$

$$+a\sum_n\left[2X_n'\left(R_m, \frac{\partial R_n}{\partial x}\right) + X_n\left(R_m, \frac{\partial^2 R_n}{\partial x^2}\right)\right] = \qquad (13)$$

$$= \frac{I_m}{\sqrt{1-x^2}},$$

with the following designations introduced

$$I_m(x) = a\int_0^\infty \tilde{I}R_m\,dr, \ (R_n, f) = \int_0^\infty fR_n\,dr.$$

The terms in square brackets in (13) describe the interaction of normal modes during propagation in an inhomogeneous waveguide [Popov, Potekhin, 1984]. In the case of smooth variations in ionospheric parameters along the x coordinate, we can neglect the interaction of

normal modes, as well as the terms with ξ in (13) and $\sqrt{\hat{\varepsilon}}\,\dfrac{\partial^2}{\partial r^2}\left(\dfrac{1}{\sqrt{\hat{\varepsilon}}}\right)$ in the expression for $\tilde{k}^2$ in (6). Then, after introducing the notation $\vartheta_n^2=\left(ka\right)^2\tilde{\gamma}_n^2=h^2\tilde{\gamma}_n^2$, (13) can be written as

$$\frac{d^2 X_n}{dx^2}+h^2 q(x)X_n=\frac{I_n}{\sqrt{1-x^2}}, \tag{14}$$

where $q(x)=\dfrac{\tilde{\gamma}_n^2}{\sqrt{1-x^2}}$. The large parameter $h=ka\sim10^6$ allows us to use asymptotic methods to solve it. The coefficient $q(x)$ has two singular points at $x=\pm1$. An asymptotic solution is framed as follows. At first, we seek asymptotic representations for X_n in $x\in\left(-1,1-\delta\right)$ and $x\in\left(-1+\delta,1\right)$, $\delta>0$. By matching these solutions inside the overlapping region $(-1+\delta,\,1-\delta)$, we obtain the solution of (14). A solution in each of the constituent regions can be found by the reference equation method [Fedoryuk, 1983; Popov, Potekhin, 1984]. As an example, we write an expression for $X_n(\theta)$ outside the transmitter and the antipode point for a point vertical magnetic dipole with current density distribution

$$j_\varphi\left(r,\theta\right)=-\frac{m_0 c}{\pi r b^2\left(1-\cos^2\theta_0\right)}\delta\left(r-b\right)\delta\left(\theta-\theta_0\right), \tag{15}$$

where m_0 is the total magnetic moment; b is the radial coordinate of the transmitter; θ_0 is the angular radius of the frame. The expression for $X_n(\theta)$ has the form

$$X_n\left(\theta\right)=\sqrt{2\pi h}\,\frac{hm_0 e^{i\pi/4}}{b^2}\times$$
$$\times\frac{\tilde{\gamma}_n\left(0\right)}{\sqrt{\tilde{\gamma}_n\left(\theta\right)}}\sqrt{\sin\theta}\,R_n\left(b,0\right)e^{ih\int_0^\theta \tilde{\gamma}_n(\theta')d\theta'}. \tag{16}$$

Similarly, for the vertical electric dipole with current density distribution

$$j_r\left(r,\theta\right)=-\frac{i\omega}{2\pi}\frac{p_0}{r^2\sin\theta}\delta\left(r-b\right)\delta\left(\theta\right), \tag{17}$$

where p_0 is the total dipole moment, the expression for $X_n(\theta)$ has the form

$$X_n\left(\theta\right)=-\sqrt{2\pi h}\,\frac{hp_0 e^{i\pi/4}}{b^2\sqrt{\varepsilon\left(b,0\right)}}\times$$
$$\times\frac{\tilde{\gamma}_n\left(0\right)}{\sqrt{\tilde{\gamma}_n\left(\theta\right)}}\sqrt{\sin\theta}\,R_n\left(b,0\right)e^{ih\int_0^\theta \tilde{\gamma}_n(\theta')d\theta'}. \tag{18}$$

Using (12), (16), and (18), taking into account the substitutions of the variable and functions, we obtain expressions for the electromagnetic field components E_φ, B_φ

$$E_\varphi\left(r,\theta\right)=\frac{A^m}{\sqrt{\sin\theta}}\times$$
$$\times\sum_n\frac{\tilde{\gamma}_n\left(0\right)R_n\left(b,0\right)}{b^2 r}\left[\frac{R_n\left(r,\theta\right)}{\sqrt{\tilde{\gamma}_n\left(\theta\right)}}\right]e^{ih\int_0^\theta \tilde{\gamma}_n(\theta')d\theta'}, \tag{19}$$

$$B_\varphi\left(r,\theta\right)=\frac{A^e}{\sqrt{\sin\theta}}\sum_n\frac{\tilde{\gamma}_n\left(0\right)R_n\left(b,0\right)}{b^2 r}\times$$
$$\times\left[-\sqrt{\varepsilon\left(r,\theta\right)}\frac{R_n\left(r,\theta\right)}{\sqrt{\tilde{\gamma}_n\left(\theta\right)}}\right]e^{ih\int_0^\theta \tilde{\gamma}_n(\theta')d\theta'}. \tag{20}$$

Here, $A^m=\sqrt{2\pi}h^{3/2}m_0 e^{i\pi/4}$, $A^e=\sqrt{2\pi}\dfrac{h^{3/2}p_0 e^{i\pi/4}}{\sqrt{\varepsilon\left(b,0\right)}}$.

Other electromagnetic field components are expressed in terms of E_φ, B_φ. Similar expressions for the field components are presented in the monograph [Kurkin et al., 1981], where they were derived by generalizing formulas for the spherically symmetric Earth—ionosphere waveguide in the adiabatic approximation.

RADIAL BOUNDARY VALUE PROBLEM

Rewrite radial equation (9) for a fixed angular coordinate θ as

$$\frac{d^2 R_n}{dy^2}+h^2 Q\left(y,\xi_n+i\chi_n\right)R_n=0, \tag{21}$$

where

$$Q=1-\alpha q_1\left(y\right)+i\beta q_2\left(y\right)-\frac{\xi_n+i\chi_n}{y^2},$$

$$\xi_n+i\chi_n=\tilde{\gamma}_n^2=\left(\gamma_n+i v_n\right)^2,$$

$$\alpha=\omega_e^2/\omega^2,\quad \omega_e^2=\frac{4\pi e^2 N_{\max}}{m},\quad \beta=\alpha v_{\text{eff}}\left(y_{\text{H}}\right)/\omega,$$

$$q_1\left(y\right)=q\left(y\right),\quad q_2\left(y\right)=q\left(y\right)\tilde{q}\left(y\right),$$

$q\left(y\right)$ is the electron density profile $N(y)$, normalized to unity at a maximum point; $\tilde{q}\left(y\right)$ is the profile of effective frequency of collisions with neutrals v_{eff}, normalized to unity at the lower boundary of the ionosphere $y=y_{\text{H}}$. In radial equation (21), transition to the dimensionless variable $y=r/a$ is made. Here and elsewhere in this section, we do not show the dependence of R_n on θ. Replace the conditions for the radial function R_n on the surface $r=a$ and for $r\rightarrow0$ by the Leontovich impedance boundary condition [Leontovich, Fok, 1946] on the Earth surface, which has the form [Kurkin et al., 1981]

$$\left[\frac{dR_n}{dy}+ihS\sqrt{\hat{\varepsilon}_t-\xi_n-i\chi_n}\,R_n\right]_{y=1}=0, \tag{22}$$

where $S=1$ for TE modes, $S=1/\hat{\varepsilon}_t$ for TM modes. The radiation condition at infinity

$$\lim_{y\rightarrow\infty}\left(\frac{dR_n}{dy}-ihR_n\right)=0. \tag{23}$$

The solutions of (9) satisfy normalization condition (11) for R_n. The eigenfunctions R_n of (21)–(23) with impedance boundary conditions on the Earth surface do not have this property. Next, to find the normalization constants in the radial-problem eigenfunctions, we use the

approximate condition

$$\int_1^\infty \frac{R_n^2(y)}{y^2} dy \approx 1. \tag{24}$$

Unlike the previously developed approach [Kurkin et al., 1981], the coefficient of the radial equation $Q(y, \xi_n + i\chi_n)$ takes into account the imaginary part of the complex permittivity of ionospheric plasma, as well as the complexity of the eigenvalue of the radial problem.

Look at the scheme for solving the radial problem, using the single-layer Earth—ionosphere waveguide as an example. In (21), the variable y is considered as a complex variable z. Then the solution of the radial equation is written as a WKB approximation since $h=ka\sim10^6$. Zeros of $Q(z, \xi_n + i\chi_n)$, $z_{1n} = y_{1n} + i\psi_{1n}$, and $z_{2n} = y_{2n} + i\psi_{2n}$ determine reflection points [Kurkin et al., 1981; Ponomarchuk et al., 2014]. Depending on $\tilde{\gamma}_n^2$, the lower reflection point is the Earth surface or the point $z_{1n} = \sqrt{\xi_n + i\chi_n} = \gamma_n + iv_n$. In the vicinity of the upper reflection point, z_{2n} changes sign $\mathrm{Re}Q(z, \xi_n + i\chi_n)$; therefore, from the condition $\mathrm{Re}Q(z, \xi_n + i\chi_n) = 0$ we can approximately write the expression for the real part $\xi_n = \gamma_n^2 - v_n^2$

$$\xi_n = y^2 \left[1 - \alpha q_1(y)\right]. \tag{25}$$

From (25) we can find radial coordinates of the reflection points y_{1n} and y_{2n}, as well as the boundary values ξ_n, which define the group of normal modes forming the field in the waveguide — minimum and maximum numbers of the normal modes in a series. To estimate the real part of ξ_n, choose a model electron density profile composed of two quasi-parabolas with a matching point $y_0 = (y_H + y_m)/2$, where y_H is the reduced height of the lower boundary of the ionosphere; y_m is the reduced height of F-layer maximum [Kurkin et al., 1981]. The parameters of the quasi-parabolas y_H, y_m correspond to the heights of the ionospheric layer of 90 and 300 km, the F-layer critical frequency $f_0=\omega_e/(2\pi)$ is 6 MHz. Figure 2 shows $\xi_n = y^2 \left[1 - \alpha q_1(y)\right]$ for different sounding frequencies. The intersection points of the black dashed lines corresponding to $\gamma_n^2 - v_n^2$ with ξ_n indicate the radial coordinates of reflection points. Blue lines denote the range of variation in the real part $\xi_n \in \left[\xi_{min}, \xi_{max}\right]$, i.e. a group of normal modes forming the field in the waveguide. The values of $\xi \in (1, \xi_{max})$ define a group of normal modes propagating in the above-ground waveguide (as termed by P.E. Krasnushkin [Krasnushkin, 1947]). The values $\xi_n \in (\xi_{min}, 1)$ determine the group of ground waveguide modes. The red line in Figure 2 indicates the dependence of ξ_n for a frequency equal to the F-layer critical frequency $f=f_0$. For this frequency, $\xi_{min} = 0$ (red dashed line). In the previously developed waveguide approach [Kurkin et al., 1981], the boundaries of the eigenvalue

real part were found by neglecting the imaginary part of $\hat{\varepsilon} = \left[1 - \alpha q_1(y) + i\beta q_2(y)\right]$ and the imaginary part of v_n in $Q(y, \xi_n + i\chi_n)$ of (21). Accordingly, in algorithms for calculating signal characteristics, the operating frequency exceeded the F2-layer critical frequency along the propagation path so that the condition $\mathrm{Re}Q(y, \gamma_n) > 0$ held [Kurkin et al., 1981; Altyntseva et al., 1987]. If the imaginary part of the spectral parameter v_n is taken into account, the lower limit on the operating frequency is removed since there is a solution of (25) for such frequencies.

The eigenvalues $\tilde{\gamma}_n^2 = \xi_n + i\chi_n$ of (21)–(23) in the complex plane (ξ_n, χ_n) are located in the upper half-plane since $\xi_n = \gamma_n^2 - v_n^2$, $\chi_n = 2\gamma_n v_n$. In the complex plane (γ_n, v_n), the spectral parameter values $\gamma_n + iv_n = \sqrt{\xi_n + i\chi_n}$ are in the upper right quadrant. In the range of operating frequencies lower than the F2-layer critical frequency, the real part of γ_n tends to zero with an increase in the number of the normal mode n, whereas the imaginary part of v_n rises sharply. At the same time, for a certain part of the spectrum, namely such that it still makes sense to take into account the contribution to the field in the Earth—ionosphere waveguide, the number of normal modes is quite large, of the order of several thousands [Ponomarchuk et al., 2014]. For numerical simulation of the normal mode characteristics, ξ_{min} at $f<f_0$ can be estimated from the damping condition of a divergent conical normal mode along the angular coordinate θ

$$E \sim e^{-\frac{2\pi d f}{c} v_n}, \tag{26}$$

where d is the distance to the transmitter. If we suppose that the radiation field decreases by a factor of e (the power of exponent is -1) at a distance $d=10$ km, then for $f=3$ MHz we get $v_n=0.0016$. In this spectral region $\gamma_n \ll v_n$ and for $\xi_n = \gamma_n^2 - v_n^2$, we can use the estimate $\xi_{min} \simeq -0.000025$.

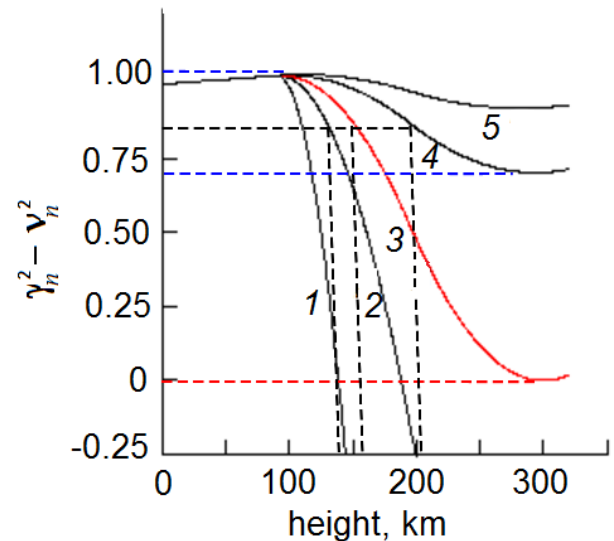*Figure 2.* Height dependence of ξ_n for different sounding frequencies of 2, 4, 6, 10, and 15 MHz (1–5 respectively)

The solution of (21) outside the vicinity of the reflection points z_{1n}, z_{2n} can be written in the form of a WKB approximation [Heading, 1965]

$$R_n(z) = \frac{C_n^{\pm}}{\sqrt[4]{Q}} \exp\left(\pm ih \int\limits_{z_{1n}}^{z} \sqrt{Q} dz \right), \tag{27}$$

where $C_n^{\pm}$ are arbitrary constants. In the region of the reflection points z_{1n}, z_{2n}, the solution of (21) is found using the standard Airy equation [Fock, 1970]. The solution of the radial boundary value problem near the Earth surface in the vicinity of $z_{1n} = \gamma_n + iv_n$ is expressed as a linear combination of Airy functions $u(x)$ and $v(x)$ [Fock, 1970], taking into account the impedance boundary conditions [Ponomarchuk et al., 2014]. Using asymptotics of the Airy functions $u(x)$ and $v(x)$, the solution of the radial problem can be transformed to a form that coincides with the WKB solution of (21),

$$R_n(z) = \frac{C_{1n}}{Q^{1/4}} \cos\left(h \int\limits_{z_{1n}}^{y} \sqrt{Q} dy + \Phi_n \right). \tag{28}$$

Here, Φ_n is an addition to the normal mode phase related to the reflection coefficient of the mode from the Earth surface [Kurkin et al., 1981; Ponomarchuk et al., 2014]. In (28), $z_{1n}=1$ for $\gamma_n<1$ and $z_{1n} = \gamma_n + iv_n$ for $\gamma_n>1$. The normal modes corresponding to $\gamma_n<1$ describe electromagnetic field propagation in the ground waveguide; and the modes with $\gamma_n>1$, in the aboveground waveguide [Krasnushkin, 1947; Kurkin et al., 1981].

For the reflection point z_{2n} in the ionosphere, we seek the solution of (21), using the standard Airy equation and choosing only the solution decreasing deep into the ionosphere [Kurkin et al., 1981; Ponomarchuk et al., 2014]. Asymptotics of the solution in the waveguide has the form [Fock, 1970]

$$R_n(z) = \frac{C_{2n}}{Q^{1/4}} \sin\left(h \int\limits_{y}^{z_{2n}} \sqrt{Q} dy + \frac{\pi}{4} \right). \tag{29}$$

From the matching condition of solutions (28) and (29) inside the waveguide, we derive an equation for the eigenvalue spectrum $\tilde{\gamma}_n^2 = \xi_n + i\chi_n$ of the radial problem and the relationship between constants C_{1n} and C_{2n}:

$$h \int\limits_{z_{1n}}^{z_{2n}} \sqrt{Q(z, \xi_n + i\chi_n, \beta)} dz +$$
$$+\Phi_n(\xi_n + i\chi_n) = \frac{\pi}{4} + \pi n, \tag{30}$$

$$(-1)^n C_{1n} = C_{2n}. \tag{31}$$

By dividing (30) into real and imaginary parts and neglecting small second-order quantities on expanding $\sqrt{Q}$ and Φ_n in small quantities of $\beta q_2(y)$ and χ_n, we obtain equations for determining ξ_n and χ_n:

$$h \int\limits_{y_{1n}}^{y_{2n}} \sqrt{Q(y, \xi_n)} dy + \operatorname{Re} \Phi_n(\xi_n) = \frac{\pi}{4} + \pi n, \tag{32}$$

$$\chi_n = \frac{h \int\limits_{y_{1n}}^{y_{2n}} \dfrac{\beta q_2(y)}{2\sqrt{Q(y, \xi_n)}} dy + \operatorname{Im} \Phi_n(\xi_n)}{h \int\limits_{y_{1n}}^{y_{2n}} \dfrac{1}{2y^2 \sqrt{Q(y, \xi_n)}} dy - \left(\operatorname{Re} \Phi_n(\xi_n) \right)'_{\xi}}. \tag{33}$$

The value of the constant C_{1n} is found from the normalization condition of radial functions (24).

MODEL OF IONOSPHERIC RADIO CHANNEL

The initial data is the radio channel characteristics and the current density distribution $\vec{j}(\vec{r}, \omega)$ in the transmitting antenna. The resulting current J_a at the output of the feeder-loaded receiving antenna located at the point $\vec{r} = (r, \theta, \varphi_F)$ is defined by the expression [Khakhinov, Kurkin, 2006; Khakhinov, 2018]

$$J_a = \sum_n A_n \left(D_n^e P_n^e e^{ih\int\limits_0^\theta \tilde{\gamma}_n^e(\theta')d\theta'} + D_n^m P_n^m e^{ih\int\limits_0^\theta \tilde{\gamma}_n^m(\theta')d\theta'} \right). \tag{34}$$

Here, $A_n = -i \dfrac{\sqrt{2\pi ka}}{c\sqrt{\gamma_n^{e,m} \sin \theta}} e^{i\frac{\pi}{4}}$. Efficiency of excitation of normal modes is characterized by $D_n^e(\varphi)$ and $D_n^m(\varphi)$. It is reasonable to call them the excitation coefficients of normal modes. Under the method of normal modes, the excitation coefficients were obtained using the reciprocity theorem [Kurkin, Khakhinov, 1984]. The coefficients $D_n^{e,m}(\varphi)$ are expressed as integrals over the volume $V_1(r_1, \theta_1, \varphi_1)$, occupied by the field source, and are analogs of antenna patterns of transmitting antennas.

$$D_n^e(\varphi) = \int\limits_{V_1} \left\{ \frac{r_1}{ika\sqrt{\varepsilon}} \frac{\partial\left(\sqrt{\varepsilon} R_n^e(r_1, \theta_1) \right)}{\partial r_1} \times \right.$$
$$\times \left[j_\theta \cos(\varphi - \varphi_1) + j_\varphi \sin(\varphi - \varphi_1) \right] +$$
$$+ j_r \tilde{\gamma}_n^e R_n^e(r_1, \theta_1) \right\} \times$$
$$\times \frac{\exp\left(-ih\tilde{\gamma}_n^e \theta_1 \cos(\varphi - \varphi_1) \right)}{r_1^2 \sqrt{\varepsilon}} adV_1, \tag{35}$$

$$D_n^m(\varphi) = \int\limits_{V_1} \left[j_\varphi \cos(\varphi - \varphi_1) - j_\theta \sin(\varphi - \varphi_1) \right] \times$$
$$\times \frac{R_n^m(r_1, \theta_1)}{r_1} \exp\left(-ih\tilde{\gamma}_n^m \theta_1 \cos(\varphi - \varphi_1) \right) dV_1. \tag{36}$$

The values $P_n^{e,m}$ characterize the current induced in the antenna by the TM- and TE-field components of individual normal modes; they can therefore be called the receiving coefficients of normal modes with corresponding polarization. Expressions for $P_n^{e,m}$ have been obtained in [Khakhinov, 2018] by the traveling-wave superposition method under conditions of applicability of the long-line theory.

$$P_n^e = \int_l \frac{Y(l)}{W} \left[(\vec{e}_r \vec{e}_l) \frac{h\tilde{\gamma}_n^e}{kr_l} R_n^e (r_l, \theta_l) - \right.$$

$$\left. - (\vec{e}_\theta \vec{e}_l) \frac{1}{ik\varepsilon} \frac{dR_n^e (r_l, \theta_l)}{dr} \right] e^{-ih\tilde{\gamma}_n^e \theta_l \cos(\varphi_F - \varphi_l)} dl, \tag{37}$$

$$P_n^m = \int_l (\vec{e}_\varphi \vec{e}_l) \frac{Y(l)}{W} R_n^m (r_l, \theta_l) e^{-ih\tilde{\gamma}_n^m \theta_l \cos(\varphi_F - \varphi_l)} dl. \tag{38}$$

Here, the function $Y(l)$ characterizes the current distribution in the antenna; W, the wire wave resistance.

The $D_n^{e,m}$ and $P_n^{e,m}$ values depend on $R_n^{e,m}(r,\theta)$ and $\left(\tilde{\gamma}_n^{e,m}\right)^2 = \left(\gamma_n^{e,m} + iv_n^{e,m}\right)^2$ of the corresponding radial boundary value problems for the magnetic TM (with index e) and electric TE (with index m) fields at transmitting and receiving points. Expression (34) is written in the adiabatic approximation under the assumption that ionospheric parameters vary smoothly along the angular coordinate θ. In this approximation, the normal mode number n is an adiabatic invariant, and the mode characteristics, determined by $\left(\tilde{\gamma}_n^{e,m}\right)^2 (\theta)$, depend on range [Kurkin et al., 1981].

Note also that the expression for the current in the receiving antenna is obtained in the isotropic Earth — ionosphere waveguide, without taking into account the magnetic field, so the sounding wave polarization type is not determined. The current in the receiving antenna is defined by the efficiency of excitation and reception of normal modes.

SIGNAL WAVEFORM

Write the signal U_a at the receiver input as

$$U_a = J_a R_a, \tag{39}$$

where R_a is the active component of the antenna (receiver) impedance. Expression (34) for J_a at the output of the receiving antenna can be rewritten as [Khakhinov, 2006]

$$J_a = i \frac{4\pi}{c} \kappa a \sum_n \left(G_n^e D_n^e P_n^e + G_n^m D_n^m P_n^m \right). \tag{40}$$

Here, the functions

$$G_n^{e,m} = -\frac{1}{4} \left(\frac{2}{\pi k a \gamma_n^{e,m} \sin\theta} \right)^{1/2} e^{ih\int_0^\theta \tilde{\gamma}_n^{e,m}(\theta')d\theta' + i\frac{\pi}{4}}. \tag{41}$$

In a homogeneous waveguide, the expression for $G_n^{e,m}$ coincides with the expression for the angular-operator Green function [Bremmer, 1949]. Thus, the expression for the current at the output of the receiving antenna within the waveguide approach is written as a series of the sum of the products of angular-operator Green functions corresponding to different radial problem eigenvalues, excitation coefficients, receiving coefficients of individual normal modes for TM and TE fields.

The current density distribution $\vec{j}(\vec{r}, \omega)$, included in the expressions for $D_n^{e,m}(\varphi)$, can be represented as

$$\vec{j}(\vec{r}, \omega) = \vec{j}_T(\vec{r}) g(\omega), \tag{42}$$

where $\vec{j}_T(\vec{r})$ is the spatial distribution of the current density in the antenna; $g(\omega)$ is the transmitted signal spectrum. By introducing new functions $D_n^{e,m} = g(\omega)\tilde{D}_n^{e,m}$, $\tilde{P}_n^{e,m} = R_a P_n^{e,m}$ and writing U_a as

$$U_a = g(\omega) H(\omega), \tag{43}$$

we obtain an expression for the transfer function of the ionospheric radio channel

$$H(\omega) = i \frac{4\pi}{c} \kappa a \sum_n \left(G_n^e \tilde{D}_n^e \tilde{P}_n^e + G_n^m \tilde{D}_n^m \tilde{P}_n^m \right). \tag{44}$$

Transition to the time dependence of the signal at the receiver input is made through the Fourier transform:

$$u_a(t) = \int_{-\infty}^{\infty} g(\omega) H(\omega) e^{-i\omega t} d\omega. \tag{45}$$

Write first the expression for the transfer function $H(\omega)$ in the form

$$H(\omega) = \sum_n H_n(\omega) = \sum_n a_n(\vec{r}, \omega) e^{i\Psi_n(\theta, \omega)}. \tag{46}$$

Here,

$$a_n(\vec{r}, \omega) =$$
$$= A_n \left[\tilde{D}_n^e(\varphi) \tilde{P}_n^e(\varphi_F) + \tilde{D}_n^m(\varphi) \tilde{P}_n^m(\varphi_F) \right] \times$$
$$\times e^{-h\int_0^\theta \left[(v_n^e + v_n^m)/2 \right] d\theta'}$$

is the amplitude multiplier; $\Psi_n(\theta, \omega) = h\int_0^\theta \gamma_n d\theta'$ is the normal mode phase. For transmission of a quasi-monochromatic pulse

$$g(t) = g_0(t) \cos(\omega_0 t + \delta), \tag{47}$$

where $g_0(t)$ is the signal envelope, the expression for $u_a(t)$ can be written as [Kurkin et al., 1981]

$$u_a(t) = \text{Re} \sum_n g_0(t - \tau_n(\theta)) H_n(\omega_0) e^{-i\omega_0 t - i\delta}, \tag{48}$$

where $\tau_n(\theta)$ is the group delay of a normal mode.

Modulation of another type used in ionosondes and radio engineering systems is the chirp signal [Ivanov et al., 2003]:

$$g(t) = \cos(\omega_0 t + \eta t^2 / 2), \tag{49}$$

where η is the rate of frequency deviation. The expression for the recorded chirp signal spectrum in analog ionosondes can be written as [Davydenko et al., 2002]

$$S_k(s) = \frac{\pi}{2} \sum_n \hat{A}(s - \tau_n) H_n(\omega_k). \tag{50}$$

Here, $s = \Omega / \eta$, where Ω is the variable of the spectrum analyzer; $\hat{A}(s)$ is the time window spectrum; $\omega_k = \omega_0 + \eta t_k$, where t_k is the time sample center. The result of processing of an individual time sample of a received chirp signal is equivalent to radio channel sounding with a complex narrowband pulsed signal. The

characteristics of this signal are determined by the time window that selects the samples.

In the ISTP SB RAS digital chirp ionosonde [Podlesny et al., 2013], signals are recorded under the scheme of recovery of the radio-channel transfer function [Podlesnyi et al., 2014]. The expression for the result of processing of received signal has the form

$$u_a(t) = H(\omega_0 + \eta t). \tag{51}$$

To construct an ionogram, digital signal samples that correspond to the expected delays in recorded signal arrival are multiplied by a smooth short time function (time window) followed by calculation of the product spectrum. As with signal processing in the analog chirp ionosonde, the received spectrum is a response of the radio channel to an effective narrowband complex signal whose shape as a function of time is equal to the shape of the window spectrum, and the carrier frequency is related through the frequency deviation rate to the position of the window in the time sweep.

NUMERICAL SIMULATION

Consider a numerical scheme for modeling the HF-radio channel characteristics, using of a sounding pulse signal as an example. Write an expression for the recorded signal at the receiver input in the form

$$u_a(\vec{r}, t) = w(\vec{r}, t) e^{iW(\vec{r}, t)} =$$
$$= \mathrm{Re} \sum_{n=n_1}^{n=n_m} \left[a_n(\vec{r}, \omega_0) g_0(t - \tau_n(\theta)) e^{i\Psi_n(\theta, \omega_0)} \right] \times \tag{52}$$
$$\times e^{-i\omega_0 t}.$$

The summation limits in (52) are selected from the conditions of effective excitation of normal modes (n_1) and reflection from the ionosphere (n_m) and are calculated from equation for normal-mode spectrum (32). The boundaries of the real part of ξ_1 and ξ_{min}, which correspond to the limits of summation n_1 and n_m, are found from (25) from the condition of existence of the Earth—ionosphere waveguide: $\mathrm{Re}\, Q(z, \xi_n + i\chi_n) > 0$. Taking into account the imaginary part of the ionosphere permittivity and the imaginary part of χ_n in the radial problem coefficient $Q(z, \xi_n + i\chi_n)$ allowed us to expand the frequency range of modeling the signal characteristics for analyzing extended inhomogeneous HF radio paths. The transmission frequency may be lower than the F2-layer critical frequency along the propagation path since there is a solution of (25) taking into account the imaginary part v_n of the spectral parameter.

The field of a single normal wave is distributed throughout the waveguide section and depends on its global characteristics, whereas the total field is localized near the ray path, where the stationarity condition of individual wave groups holds [Potekhin, Orlov, 1981]. For a ground receiver, the stationarity condition takes the form

$$\Delta\Psi_n(\theta, f) = \frac{1}{2\pi}(\Psi_n - \Psi_{n+1}) = l, \tag{53}$$

where l is an integer, $f = \omega_0 / (2\pi)$. The ray elevation angle ϕ_1 from the point y_b is related to the spectral parameter of the central wave of the group of phased waves with the number n_i by $\cos\phi_1 = \gamma_{n_i}(0) / y_b$. Then l is the number of signal reflections from the ionosphere.

Expressions (52) and (53) serve as the formula basis for the scheme for calculating the distribution of decameter signal field in the Earth—ionosphere waveguide by the method of normal modes. At the first stage, we calculate the normal mode characteristics a_n, Ψ_n, τ_n, $\Delta\Psi_n$ at reference points of the spectrum. The spectrum of normal modes $\tilde{\gamma}_n^2 = \xi_n + i\chi_n$ is found from the solution of transcendental equation (32) and equation (33). The real γ_n and imaginary v_n parts of the spectral parameter $\tilde{\gamma}_n$ are determined from $\xi_n = \gamma_n^2 - v_n^2$, $\chi_n = 2\gamma_n v_n$. The profiles of electron density $N(y)$ and effective collision frequency $v_{\mathrm{eff}}(y)$, calculated from the ionosphere model, and the underlying medium parameters from the global model of electrical properties of the Earth surface are used as input data [Ponomarchuk, 1984]. The normal mode groups forming the signal field at the receiving point for waveguide channels E, F1, and F2 are identified. At the second stage, the solution of (53) with respect to the number n allows us for each of E, F1, and F2 waveguide channels to determine the signal mode structure (the number of signals and their identification) and to calculate the time and angular characteristics of signals for propagation modes.

Maxima $\Delta\Psi_n(\theta, f)$ depending on the number n define the maximum usable frequencies (MUF) of propagation modes and the skip zone border along the Earth surface for each of E, F1, and F2 waveguide channels. Solution of

$$\max_{n \in [n_1, n_m]} \Delta\Psi_n(\theta, f) = l \tag{54}$$

with respect to f for fixed θ determines MUF of the l-hop. The solution of (54) with respect to θ for a fixed frequency f defines the distance to the skip zone border of the l-hop.

Figure 3 presents the oblique incidence ionogram along the Cyprus—Irkutsk path, obtained on January 1, 2023 at 04:45 UT, and the results of modeling of distance-frequency characteristics of signals. The calculations were carried out using the IRI-2016 model [Bilitza et al., 2017]. The Cyprus—Irkutsk path 5690 km long runs in midlatitudes; the propagation conditions corresponded to quiet heliogeophysical conditions. The input data in the algorithm for calculating signal characteristics was the profiles of electron density and electron-neutral collision frequency, calculated with the discrete of ~ 200 km along the propagation path. The distance characteristics of oblique sounding signals were calculated by solving stationarity equation (53) with respect to the central numbers n_i of groups of phased normal modes, which make the main contribution to the field at the receiving point. The number n_i is related to the angle of arrival of the path ϕ_2 at the receiving point by $\cos\phi_2 = \gamma_{n_i}(\theta) / y$. For the specified sounding frequency f and distance D for each of E, F1, and F2 channels, there are two solutions of (53) corresponding
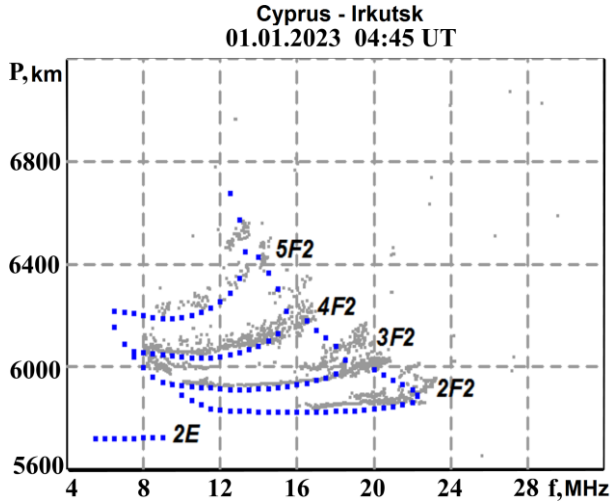
Figure 3. OS ionogram and results of simulation of distance-frequency characteristics of OS signals on January 1, 2023 at 04:45 UT. Gray dots denote the OS ionogram; blue dots, the simulation results
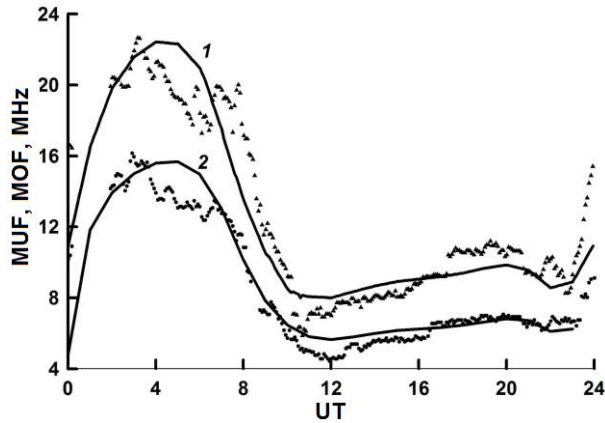

Figure 4. Daily variations in calculated MUF (solid lines) and experimental MOF (triangles and circles) for the Magadan — Irkutsk path on January 16, 2010; 1 — 1F2; 2 — 2F2

to different angles of arrival of the propagation path of phased normal mode packet — lower and upper beams. The group path of signal propagation is equal to $c\tau_{n_i}(\theta)$.

With increasing frequency, the propagation trajectories approach each other and intersect at MUF of the propagation mode. MUF can be found from the solution of (54). Figure 3 shows calculation results only for propagation modes 2E, 2F2, 3F2, 4F2, and 5F2. For the selected moment of time, the predicted F2-layer critical frequency along the Cyprus—Irkutsk propagation path varied from 5.5 to 9.1 MHz, it would be, therefore, impossible to run the simulation in the lower part of the range below 8 MHz without the waveguide method modification considered.

Figure 4 illustrates daily variations in calculated MUF and experimental maximum observed frequencies (MOF) along the Magadan—Irkutsk path for January 16, 2010.

The results of calculation of MUF for propagation modes 1F2 and 2F2 are plotted with solid lines 1 and 2 respectively. The experimental MOF values are marked with triangles and circles. MUF in waveguide channel F2 was calculated by solving (54) with respect to *f* for fixed

coordinates of the receiving point.

Amplitude characteristics of signals are calculated using (52) according to the scheme described in [Kurkin et al., 1986]. The recorded signal envelope $w(\vec{r}, t)$ is calculated through the direct numerical summation of expressions of the form

$$w(\vec{r}, t) == \left[\left(\sum_{n=n_1}^{n=n_m} a_n g_0(t - \tau_n)\cos\Psi_n \right)^2 + \left(\sum_{n=n_1}^{n=n_m} a_n g_0(t - \tau_n)\sin\Psi_n \right)^2 \right]^{1/2}. \quad (55)$$

Calculating $w(\vec{r}, t)$ makes it possible to investigate the received signal waveform for both separated and time-overlapping pulses, i.e. both in the lit zone and in the caustic region, where the upper and lower beams merge. The signal envelope in the center of the pulse of a signal corresponding to the delay $\tau_{n_i} + T/2$ can be taken as the signal amplitude. Note that the amplitude characteristics of signals are calculated for specified receiving and transmitting antenna-feeder devices, taking into account the type of transmitted signal modulation.

Figures 5 and 6 present the results of calculation of the range-time distribution of the pulse signal field envelope in the vicinity of the skip zone border D_0 for the 10 MHz frequency for medium-wet soil and sea surface respectively. The transmitter is a point vertical dipole. The transmitter power is 1 kW; the total duration of the transmitted pulse is 140 μs; the distance is calculated with respect to D_0=1108.25 km. The signal amplitude oscillates both in time and with distance away from D_0 to the lit zone. In the shadow zone for $D<D_0$, the signal envelope features two small amplitude maxima. These signals are analogous to the edge rays of the space-time theory of pulse diffraction. When moving into the lit zone, the signal amplitude increases almost exponentially [Kurkin et al., 1982; Bremmer, 1949], whereas the maximum in the amplitude profile is shifted in range relative to D_0 toward the skip zone. At ~8–10 km distance from D_0 (see Figure 6), the signal begins to split into two similar waveforms, which are completely separated at some distance away (depending on pulse duration).

Figure 7 shows the range dependence of the average signal amplitude in the vicinity of D_0=1108.25 km. To reveal the dynamics of the average signal amplitude, the pulse duration was taken to be 440 μs. The signal amplitude oscillates due to the interference of the lower and upper beams. With increasing sounding frequency, the oscillation period of the average amplitude increases. Accordingly, the distance increases from the skip zone border D_0 at which the signal is divided into two signals corresponding to the lower and upper beams. The size of the interference region of 440 μs pulse signals occupies a range of ~17 km for the 10 MHz frequency and ~25 km for 12 MHz. The signal amplitude dynamics near the skip zone border, obtained by analyzing coherent properties of a number of normal modes, is discussed in more detail in [Kurkin et al., 1982].
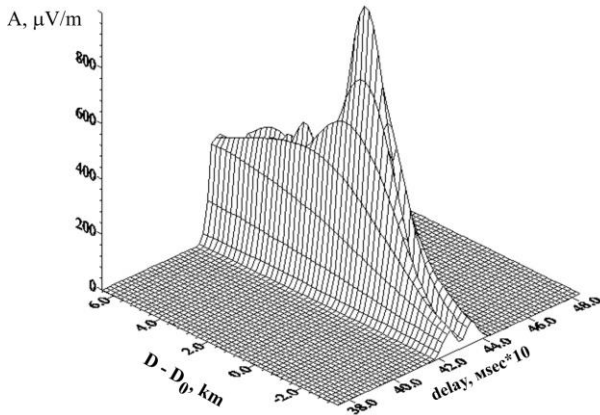
Figure 5. Range-time distribution of the signal envelope near the skip zone border for medium-wet soil
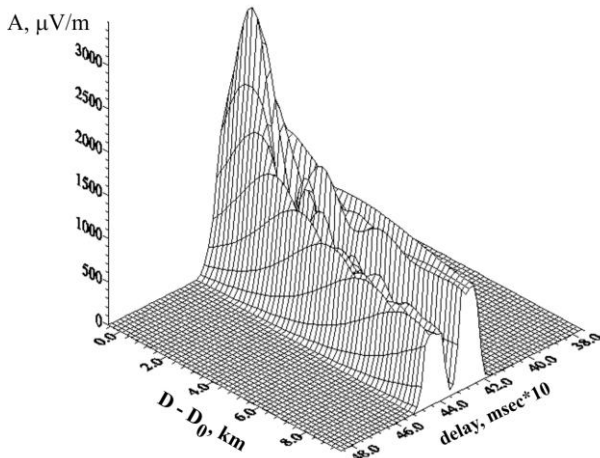

Figure 6. Range-time distribution of the signal envelope near the skip zone border for the sea surface
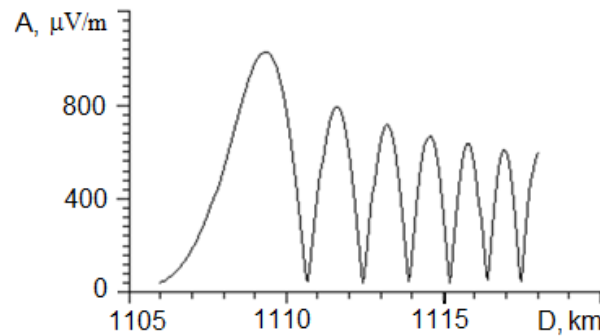

Figure 7. Range dependence of signal amplitude in the vicinity of the skip zone border

The developed algorithms for simulating the space-time structure of the incident signal field provide a basis for the scheme for calculating characteristics of signals scattered by the roughness of the Earth surface during backscatter sounding (BS) of the ionosphere [Ponomarchuk et al., 2022].

Figure 8 presents the results of modeling the envelopes of one-hop BS signals for November 08, 2020, 01:00 UT. The transmitter is in Usolye-Sibirskoye (52.8° N, 103.3° E); the receiver, in Tory village, Republic of Buryatia (51.8° N, 103° E). The sounding azimuth is 55°. Input parameters of the algorithm are the
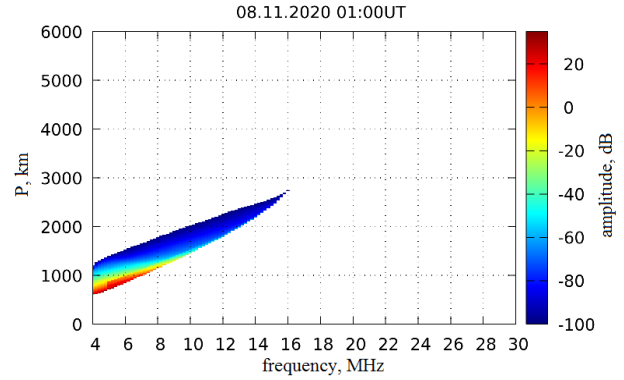
Figure 8. Results of simulation of BS signal envelopes for November 08, 2020, 01:00 UT

profiles of electron density and effective collision frequency, calculated using the IRI–2016 model, electrical parameters, and coefficients of scattering by the Earth surface [Ponomarchuk, 1984; Ishimaru, 1981; Chernov, 1971]. Under the waveguide approach, characteristics of BS signals are simulated on the basis of the incoherent scattering approximation, in which the scattered field characteristics are expressed through the incident field characteristics (angle of incidence, amplitude) and a local scattering diagram or scattering coefficient. The amplitude characteristics of BS signals, including the time sweep, are calculated by sweeping all beams from the lit area at each given moment of time. It is assumed that the BS signal field is formed by scattered signals arrived at the receiver along the same possible paths along which sounding signals propagate. Amplitudes of the signals arrived at the receiver at a given time are summed incoherently. The amplitude characteristics of BS signals are simulated for the specified receiving-transmitting antenna-feeder devices. The BS signal in the synthesized ionogram shown in Figure 8 is formed by scattered signals arriving at the receiver along one-hop paths through reflection from the F2 layer.

A characteristic feature of the BS ionograms is the presence of a pronounced leading edge — the minimum group path of arrival of scattered signals from the skip zone border. From the solution of (53) and (54) we have developed near real-time algorithms for calculating the minimum group propagation path and the distance to the skip zone border, which are employed in the scheme for determining the leading edge of signals in BS ionograms [Ponomarchuk et al., 2022].

CONCLUSION

Under the waveguide approach, we have presented a composite model of HF radio channel, including transmitting and receiving devices, an ionospheric radio channel, and a software package for calculating radio signal characteristics. We have represented the radio-channel transfer function as a series of products of angular-operator Green functions, excitation coefficients, and receiving coefficients of individual normal modes for TM and TE fields. With the method of normal modes, we have modified the scheme for solving the radial problem and constructing the radial-operator spectrum, taking into account absorption of the signal

field in the ionosphere and on the Earth surface. This allows us to simulate the HF radio channel in the frequency range including frequencies below the F2-layer critical frequency. By analyzing and numerically summing up a number of normal modes, we have developed algorithms and programs for calculating distance-frequency, frequency-angular, and amplitude characteristics of signals, including time sweep of signal. Electron density profiles, the effective collision frequency, electrical parameters of the underlying medium along a radio path, and parameters of antenna-feeder devices are set as input data.

REFERENCES

Ahluwalia D.S., Keller J.B. Exact and asymptotic representations of the sound field in a stratified ocean. *Wave Propagation and Underwater Acoustics. Springer, Berlin, Heidelberg.* 1977, pp. 14–85. DOI: 10.1007/3-540-08527-0_2.

Aizenberg G.Z., Belousov S.P., Zhurbenko E.M. *Shortwave antennas*. Moscow, Radio and communication Publ., 1985, 536 p. (In Russian).

Altyntseva V.I., Ilyin N.V., Kurkin V.I. Simulation of a decameter radio channel based on the method of normal waves. *Technique of communication facilities. SS ser.* Moscow: Ekos Publ., 1987, iss. 5, pp. 28–34. (In Russian).

Anderson S. Cognitive HF radar. *J. Eng.* 2019, vol. 2019, iss. 20, pp. 6772–6776. DOI: 10.1049/joe.2019.0537.

Avdeev V.B., Demin A.V., Kravtsov Yu.A., Tinin M.V., Yarygin A.P. The interferential integral method (review) *Radiophys Quantum Electron*. 1988, vol. 31, pp.907–921.

Ayliffe J.K., Durbridge L.J., Frazer J.F., Gardiner-Garden R.S., Heitmann A.J., Praschifka J., et al. The DST Group High-Fidelity, Multichannel Oblique Incidence Ionosonde. *Radio Sci*. 2019, vol. 54, no. 1, pp. 104–114. DOI: 10.1029/2018RS006681.

Barabashov B.G., Vertogradov G.G. Dinamic adaptive physically–structural model of ionospheric sky-wave channel. Mathematical Modeling. 1996, vol. 8, no. 2, pp. 3–18. https://www.mathnet.ru/php/agreement.phtml?option_lang=rus. (In Russian).

Baranov V.A., Popov A.V. Generalization of the parabolic equation for EM waves in a dielectric layer of nonuniform thickness. *Wave Motion*. 1993, vol. 17, no. 4, pp. 337–347. DOI: 10.1016/0165-2125(93)90013-6.

Baranov V.A., Karpenko A.L., Popov A.V. Evolution of Gaussian beams in the nonuniform Earth-ionosphere waveguide. *Radio Sci*. 1992, vol. 27, no. 2, pp. 307–314. DOI: 10.1029/91RS02639.

Bilitza D., Altadill D., Truhlik V., Shubin V., Galkin I., Reinisch B., Huang X. International Reference Ionosphere 2016: From ionospheric climate to real-time weather predictions. *Space Weather*. 2017, vol. 15, no.2, pp. 418-429.

Bremmer H. *Terrestrial Radio Waves*. Theory of Propagation, Amsterdam, 1949, 343 p.

Cherkashin Yu.N. Application of parabolic equation method for calculation wavefields in inhomogeneous media *Radio Engineering and Electronic Physics*. 1971, vol. 16, no. 1, pp. 173–174. (In Russian).

Chernov Yu.A. *Backscatter sounding ionosphere*. Moscow, Svyaz Publ.,1971, 204 p. (In Russian).

Davydenko M.A., Ilyin N.V., Khakhinov V.V. On the shape of measured spectra of the ionosphere sounding by an FMCW signal under dispersion case. *J. Atmos. Solar-Terr. Phys.* 2002, Vol. 64, no. 17, pp. 1897–1902. DOI: 10.1016/S1364-6826(02)00196-7.

Fedoryuk M.V. *Asymptotic methods for linear ordinary differential equations*. Moscow, Nauka Publ., 1983, 352 p. (In Russian).

Fock V. A. *Problems of diffraction and propagation of electromagnetic waves*. Moscow, Sov. Radio Publ. 1970, 520 p. (In Russian).

Ginzburg V.L. *Propagation of Electromagnetic Waves in Plasmas*. New York: Pergamon Press. 1964.

Gurevich A.V., Tsedilina E.E. *Long distance propagation of HF radio waves*. Berlin: Springer-Verlag, 1985.

Heading D. *Introduction to the method of phase integrals (WKB method)*. Moscow, Mir Publ., 1965, 240 p. (In Russian).

Ipatov E.B., Lukin D.S., Palkin E.A. Numerical realization of the Maslov canonical operator method for problems of shortwave radio propagation in the ionosphere of the earth. *Radiophysics and Quantum Electronics*. 1990, vol. 33, no. 5, pp. 411–420. DOI: 10.1007/BF01045406.

Ipatov E.B., Kryukovskii A.S., Lukin D.S., Palkin E.A., Rastyagaev D.V. Methods of simulation of electromagnetic wave propagation in the ionosphere with allowance for the distributions of the electron concentration and the Earth's magnetic field. *J. Commun. Technol. Electron*. 2014, vol. 59, no. 12, pp. 1341–1348. DOI: 10.1134/S1064226914120079.

Ishimaru A. *Wave propagation and scattering in random media*. Academic press, New York, 1978, 250 p.

Ivanov D.V., Ivanov V.A., Ovchinnikov V.V., Elsukov A.A., Ryabova M.I. Adaptive wideband equalization for frequency dispersion correction in HF band considering variations in interference characteristics and ionosphere parameters. *ITM Web Conf*. 2019a, vol. 30, no. 15021, pp. 1–6. DOI: 10.1051/itmconf/20193015021.

Ivanov V.A., Ivanov D.V., Ryabova N.V., Ryabova M.I., Chernov A.A., Ovchinnikov V.V. Studying the parameters of frequency dispersion for radio links of different length using software-defined radio based sounding system. *Radio Sci*. 2019b, vol. 54, no. 1, pp. 34–43. DOI: 10.1029/2018RS006636.

Ivanov V.A., Kurkin V.I., Nosov V.E., Uryadov V.P., Shumaev V.V. Chirp ionosonde and its application in the ionospheric research. *Radiophysics and Quantum Electronics*. 2003, vol. 46, iss. 11, pp. 821–851.

Kamel A., Felsen L. B. On the ray equivalent of a group of modes. *The Journal of the Acoustical Society of America*. 1982, vol. 71, no. 6, pp. 1445–1452. DOI: 10.1121/1.387841.

Kazantsev A.N., Lukin D.S., Spiridonov Yu.G. A method for studying the propagation of radio waves in an inhomogeneous magnetoactive ionosphere. *Space Res*. 1967, vol. 5, no. 4, pp. 593–600. (In Russian).

Khakhinov V.V. Receiving antenna electrodynamic model in terms of waveguide representation of HF field. *Solar-Terr. Phys*. 2018, vol. 4, iss. 3, pp. 92–95. DOI: 10.12737/stp-43201812.

Khakhinov V.V., Kurkin V.I. Waveguide approach to modeling of the ionosphere radiochannel. *Proc. of the 11-th Inter. Conf. on Mathematical Methods in Electromagnetic Theory MMET-2006, IEEE: 06EX1428. Kharkiv, Ukraine*. 2006, pp. 284–286. DOI: 10.1109/MMET.2006.1689693.

Krasnushkin P.E. *The method of normal waves as applied to the problem of long-distance radio communications*. Moscow: Publishing House of Moscow State University. 1947, 52 p. (In Russian).

Krasnushkin P.E., Yablochkin N.A. *Theory of propagation of superlong waves*. Moscow, Computing Center of the Academy of Sciences of the USSR Publ., 1963, 94 p. (In Russian).

Kravtsov Yu.A., Orlov Yu.I. *Geometrical Optics of Inhomogeneous Media*. Springer, Berlin. 1990.

Kryukovskii A.S., Lukin D.S., Palkin E.A., Rastyagaev D.V Wave catastrophes: Types of focusing in diffraction and propagation of electromagnetic waves. *J. Commun. Technol. Electron.* 2006, vol. 51, no. 10, pp. 1087–1125. DOI: 10.1134/S1064226906100019.

Kurkin V.I., Khahinov V.V. On the excitation of a spherical waveguide Earth-ionosphere by an arbitrary current distribution. *Research on Geomagnetism, Aeronomy and Solar Physics.* Moscow, Nauka Publ., 1984, iss. 69, pp. 16–22. (In Russian).

Kurkin V.I., Orlov I.I., Popov V.N. *Normal Wave Technique in HF Radio Communication Problem*. Moscow, Nauka Publ., 1981. (In Russian).

Kurkin V.I., Orlov A.I., Orlov I.I, Popov V.N., Potekhin A.P. Investigation of the envelopes of a pulsed HF signal in the vicinity of a caustic based on the method of normal waves. *Research on Geomagnetism, Aeronomy and Solar Physics*. Moscow: Nauka Publ., 1982, iss. 60, pp. 198–205. (In Russian).

Kurkin V.I., Orlov A.I., Orlov I.I. Scheme for calculating the characteristics of a pulsed decameter radio signal based on the numerical summation of normal waves. *Research on Geomagnetism, Aeronomy and Solar Physics.* M.: Nauka Publ., 1986, iss. 75, pp. 159–164. (In Russian).

Leontovich M.A., Fok V.A. Solving the problem of propagation of electromagnetic waves along the surface of the Earth using the parabolic equation method. *J. Experimental and Theoretical Physics*. 1946, vol. 16, no. 7, pp. 557–573. (In Russian).

Lukin D.S., Spiridonov Yu.G. Application of the method of characteristics for the numerical solution of problems of radio wave propagation in an inhomogeneous and nonlinear medium. J. Communications Technology and Electronics. 1969, vol. 14, no. 9, pp. 1673–1677. (In Russian).

Makarov G.I., Novikov V.V., Rybachek S.T. *Propagation of Radio Waves in the Earth-Ionosphere Waveguide Channel and in the Ionosphere*. Moscow, Nauka Publ., 1993, 148 p. (In Russian).

Podlesnyi A.V., Brynko I.G., Kurkin V.I., et al. Multifunctional chirp ionosonde for monitoring the ionosphere. *Heliogeophys. Res.* 2013, no. 4, pp. 24–31. (In Russian).

Podlesnyi A.V., Lebedev V.P., Ilyin N.V., Khahinov V.V. Implementation of the method for restoring the transfer function of the ionospheric radio channel based on the results of sounding the ionosphere with a continuous chirp signal. *Electromagnetic waves and electronic systems*. 2014, vol. 19, no. 1, pp. 63–70. (In Russian).

Ponomarchuk S.N. Model of the electrical properties of the earth's surface in the HF range. *Research on Geomagnetism, Aeronomy and Solar Physics.* Moscow, Nauka Publ., 1984, iss. 69, pp. 42–47. (In Russian).

Ponomarchuk S.N., Ilyin N.V., Penzin M.S. The model of radio wave propagation in frequency range 1–10 MHz on the base of normal wave technique. *Solar-Terr. Phys.* 2014, iss. 25, pp. 33–39. (In Russian).

Ponomarchuk S.N., Grozov V.P., Ilyin N.V., Kurkin V.I., Oinats A.V., Penzin M.S., et al. Backscatter Ionospheric Sounding by a Continuous Chirp Signal. *Radiophysics and Quantum Electronics*. 2022, vol. 64, iss. 8-9, pp. 591–604. DOI: 10.1007/s11141-022-10162-7.

Popov V.N., Potekhin A.P. On the propagation of decameter radio waves in the azimuth-symmetric "Earth-ionosphere" waveguide. *Research on Geomagnetism, Aeronomy and Solar Physics.* Moscow, Nauka Publ., 1984, iss. 69, pp. 9–15. (In Russian).

Potekhin A.P., Orlov I.I. Approximate summation formula for a series of normal waves. *Research on Geomagnetism, Aeronomy and Solar Physics.* Moscow, Nauka Publ., 1981, iss. 57, pp. 135–137. (In Russian).

Zernov N.N., Gherm V.E., Zaalov N.Yu., Nikitin A.V. The generalization of Rytov's method to the case of inhomogeneous media and HF propagation and scattering in the ionosphere. *Radio Sci.* 1992, vol. 27, no. 2, pp. 235–244. DOI: 10.1029/91rs02920.

URL: http://ckp-rf.ru/ckp/3056/ (accessed June 2, 2023).